Radar SINR Enhancement in Active RIS-Assisted ISAC Systems via Movable Antenna Optimization

Seungseok Sin
Department of Intelligent Electronics and Computer Engineering
Chonnam National University
Gwangju, Republic of Korea
ssskit7@naver.com

Insik Cho
Department of Intelligent Electronics and Computer Engineering
Chonnam National University
Gwangju, Republic of Korea
dr-cho@jnu.ac.kr

Kyunam Kim
Alps Electric Korea Co., Ltd.
Gwangju, Republic of Korea
kyunam.kim@kr.alps.com

Huaping Liu
Oregon State University
United States of America
huaping.liu@oregonstate.edu

Sangmi Moon
Department of IT Artificial Intelligence
Korea Nazarene University
Cheonan, Republic of Korea
moonsm@kornu.ac.kr

Intae Hwang
School of Electronics and Computer Engineering and Department of Intelligent Electronics and Computer Engineering
Chonnam National University
Gwangju, Republic of Korea
hit@jnu.ac.kr

***Abstract*— This paper investigates an active reconfigurable intelligent surface (RIS) and movable antenna (MA)-aided integrated sensing and communication (ISAC) system for non-terrestrial networks. To enhance radar sensing performance, an SCA-based optimization framework is developed to adapt MA positions under communication quality-of-service constraints. Simulation results demonstrate that the proposed MA-enabled scheme significantly improves radar SINR compared with fixed antenna arrays, achieving comparable performance with fewer antenna elements.**

***Keywords*— Line-of-sight (LOS), integrated sensing and communication (ISAC), movable antenna (MA), reconfigurable Intelligent Surface (RIS), unmanned aerial vehicle (UAV).**

I. INTRODUCTION

Next-generation 6G networks aim to integrate high-rate communication and high-resolution sensing within a unified hardware platform, known as integrated sensing and communication (ISAC) [1], [2-5]. ISAC simultaneously transmits data and radar waveforms over the same spectrum, thereby improving spectral and energy efficiencies.

Movable antennas (MAs) enable mechanical repositioning of antenna elements within a small region to actively exploit spatial diversity [6]. MAs enhance channel adaptability and maintain stable links even under blockages or non-LoS conditions, rendering MAs particularly suitable for unmanned aerial vehicle (UAV)-based non-terrestrial ISAC systems [6].

Studies have mostly focused on passive RISs or fixed arrays and limited the optimization to either sensing or communication objectives. The optimization MAs within ISAC has not been systematically studied. This study addresses this research gap by proposing an optimization framework that tunes position parameters to maximize radar SINR while satisfying the quality of service (QoS) constraints of communication.

II. SYSTEM MODEL AND CHANNEL MODEL

This study investigates an ISAC architecture that jointly employs an active RIS and MAs. As depicted in Fig. 1, the considered scenario consists of a BS equipped with M MA elements, a UAV carrying an active RIS, a radar target, and multiple single-antenna users. For simplicity, the ISAC BS and UAV-mounted RIS are denoted as BS and RIS, respectively, throughout the paper. The MAs at the BS can relocate within a designated movement region, allowing the transceiver to adjust its spatial configuration in response to channel variations. Using this adaptive array, the BS simultaneously delivers communication signals to K users while directing sensing waveforms toward the radar target. Because the LoS path between the BS and the target is obstructed, sensing relies on the UAV-borne active RIS, which contains N reflecting elements equipped with low-noise amplifiers. By amplifying the impinging signal before re-radiation, the active RIS compensates for the severe attenuation experienced in multi-hop cascaded paths, particularly in four-hop BS–RIS–target–RIS–BS links, thereby enhancing both communication and sensing performance.

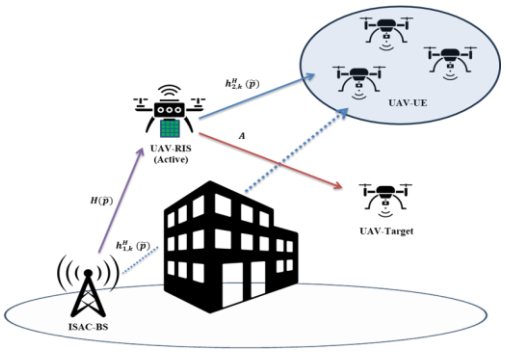

Fig. 1. System model of the active RIS and MA-aided ISAC system.

A. Transmit signal model

The transmit signal of the ISAC BS is expressed as

$$x = W_r s + W_c c = [W_r, W_c]\begin{bmatrix} s^T \\ c^T \end{bmatrix} = Wx, \quad (1)$$

where $s \in \mathbb{C}^{M\times 1}$ denotes the radar-only signal, $c \in \mathbb{C}^{K\times 1}$ represents the communication signal vector intended for K single-antenna users, and $W_r \in \mathbb{C}^{M\times M}$ and $\mathrm{W_c} \in \mathbb{C}^{\mathrm{M\times K}}$ denote the radar and communication beamforming matrices, respectively. Therefore, the overall BS beamforming matrix is given as $W = [W_r, W_c] \in \mathbb{C}^{M\times(M+K)}$. Radar signal s is generated using pseudo-random coding, satisfying $E[ss^H] = I_M$. The information signal c follows a complex Gaussian distribution, $CN(0, I_K)$. Accordingly, the covariance matrix of the transmitted waveform can be expressed as

$$R = E[xx^H] = WW^H = R_c + \sum_{k=1}^{K} R_k. \quad (2)$$

B. Channel model

To model the propagation characteristics, we employ a planar far-field approximation, as formulated in a prior study [5]. For the same propagation path, the transmit and receive links share identical angles of departure, angles of arrival, and path-gain coefficients; only the corresponding signal phases differ. The positions of the MAs are represented as $\tilde{p} = [p_1, p_2, \dots, p_M] \in \mathbb{R}^{2\times M}$, where $p_m = [x_m, y_m]^T$ denotes the coordinates of the m-th MA. The transmit and receive elevation and azimuth angles are defined as ${\theta_j}^t \in [0,\pi], {\varphi_j}^t \in [0,\pi], (1 \leqq j \leqq L_t)$ and ${\theta_i}^r \in [0,\pi], {\varphi_i}^r \in [0,\pi], (1 \leqq i \leqq L_r)$, respectively, where L_t and L_r denote the numbers of departure and arrival paths of the BS–RIS channel, respectively. The number of departure paths of the BS–user k link is indicated by ${L_t}^k$. Because the channel observed at each MA element depends on both spatial position and surrounding propagation geometry, the response of this channel varies accordingly.

Following the modeling approach reported in [5], the field-response vector associated with the MA positioned, $p = [x, y]^T$, or the BS–RIS link is given by

$$g(p) = [e^{j2\frac{\pi}{\lambda}{\rho_t}^1(p)}, \cdots, e^{j2\frac{\pi}{\lambda}{\rho_t}^{L_t}(p)}]^T \in \mathbb{C}^{L_t\times 1}, \quad (3)$$

where ${\rho_t}^j(p) = x\,sin{\theta_j}^t cos{\varphi_j}^t + y\,cos{\theta_j}^t$ represents the additional propagation distance of the j-th transmit path relative to the reference point. The aggregate field responses of the M movable antennas in the BS–RIS link are collected into matrix (4), where each column corresponds to the response of an individual MA at position p_m.

$$G(\tilde{p}) = [g(p_1), g(p_2), \dots, g(p_M)] \in \mathbb{C}^{L_t\times M}. \quad (4)$$

The corresponding matrix of the BS–user k link is

$$G_k(\tilde{p}) = [g_k(p_1), g_k(p_2), \dots, g_k(p_M)] \in \mathbb{C}^{{L_t}^k\times M}. \quad (5)$$

The field response of the RIS can be formulated in a similar manner to that of the BS array, where each reflecting element introduces a path-dependent phase shift according to the corresponding spatial coordinate. The path-response matrices of the BS–RIS and BS–user k links are denoted as $\Sigma \in C^{L_r\times L_t}$ and $\Sigma_k \in C^{{L_r}^k\times {L_t}^k}$, respectively. Hence, the channel matrix between the BS and UAV-RIS is expressed as

$$H(\tilde{p}) = F(r)^H \Sigma G(\tilde{p}) \in \mathbb{C}^{N\times M}. \quad (6)$$

Moreover, the channel between the BS and user k is denoted as ${h_{1,k}}^H(\tilde{p}) = 1^H \Sigma_k G_k(\tilde{p}) \in \mathbb{C}^{1\times M}$. The channel between the UAV-RIS and user k is denoted as ${h_{2,k}}^H \in \mathbb{C}^{1\times N}$. The channel of the RIS–target link can be approximated as follows, assuming that the radar target has a sufficiently small spatial extent (i.e., a point target).

$$A = \beta_r a(\theta_A) a(\theta_A)^H \in \mathbb{C}^{N\times N}, \quad (7)$$

where θ_A denotes the direction of arrival of the reflected signal with respect to the RIS. The steering vector of the RIS array is given by

$$a(\theta) = [1, e^{j2\pi\frac{d_{RIS}}{\lambda}sin\theta}, \dots, e^{j2\pi(N-1)\frac{d_{RIS}}{\lambda}sin\theta}]^T \quad (8)$$

where d_{RIS} represents the inter-element spacing of the RIS. In this setup, the active RIS reflects and amplifies the signals received from the BS, directing them toward the radar target and the communication users. The first reflected signal, corresponding to the amplified BS–RIS path, is expressed as

$$y_1 = QH(\tilde{p})x + Qv_1, \quad (9)$$

where $Q \in \mathbb{C}^{N\times N}$ denotes the reflection–amplification matrix of the active RIS and $v_1 \sim CN(0, \sigma^2 I_N)$ represents the additive Gaussian noise generated during the first reflection. The second reflected signal, i.e., the echo from the target re-reflected by the RIS and received at the BS, can be expressed as

$$y_2 = Q^H AQH(\tilde{p})x + Q^H AQv_1 + Q^H v_2, \quad (10)$$

where $v_2 \sim CN(0, \sigma^2 I_N)$ is the additive Gaussian noise introduced during the second reflection. To ensure the stable operation of the active RIS, its total transmit power is constrained by ${P_{RIS}}^{max}$, which satisfies

$$E[||\,y_1\,||_2{}^2 + ||\,y_2\,||_2{}^2] \leqq {P_{RIS}}^{max}. \quad (11)$$

In the considered ISAC scenario, the echo signal received at the BS contains not only the desired component reflected from the RIS–target–RIS path but also thermal noise generated at the active RIS and BS, as well as interference from the BS–RIS–BS link. Since the BS–RIS–BS link does not carry target-related information, it is regarded as interference. Accordingly, the radar echo signal received at the BS can be expressed as

$$\tilde{y_r} = H(\tilde{p})^H (y_1 + y_2) + z_r \quad (12)$$

where $z_r \sim \mathcal{CN}(0, \sigma_r^2 I_M)$ represents the additive white Gaussian noise (AWGN) at the BS. By substituting (9) and (10) into (12), the received radar signal becomes

$$\tilde{y_r} = H^H Q^H AQHx + H^H Q^H AQv_1 + H^H Q^H v_2 + H^H Q^H Hx + z_r \quad (13)$$

Let

$$B = H^H Q^H AQH \quad (14)$$

then the radar SINR can be expressed as

$$SINR = Tr(BRB^H J^{-1}) \quad (15)$$

III. Proposed Algorithm

In this subsection, we address the optimization of the MA position vector $\tilde{p}$. Given that the ISAC BS beamforming matrix W and the active RIS reflection–amplification matrix Q are fixed from the previous steps, only the MA positions are treated as optimization variables. The radar SINR expression in (16) can be rewritten as a function of $\tilde{p}$ [5]:

$$f(\tilde{p}) = Tr(B(\tilde{p})R_i B(\tilde{p})^H J(\tilde{p})^{-1}) \quad (16)$$

Therefore, at the i-th iteration, the radar SINR function is approximated by a lower-bound surrogate that preserves both the function value and gradient at the current iteration point, ensuring monotonic convergence.

$$\tilde{f}(\tilde{p} \mid \tilde{p}^i) = 2\Re Tr\left(X_i^H J_i^{-1} X(\tilde{p})\right) - Tr\left(J_i^{-1} X_i X_i^H J_i^{-1} J(\tilde{p})\right), \quad (17)$$

where $X_i = B(\tilde{p}^{(i)})W$. As $B(\tilde{p}) = H(\tilde{p})^H SH(\tilde{p})$, with $S = Q^H AQ$, the first-order variation of $B(\tilde{p})$ with respect to the change, $\Delta\tilde{p}$, in antenna position is expressed as

$$dB = (dH)^H SH_i + H_i^H S(dH), \quad (18)$$

where $H_i = H(\tilde{p}^{(i)})$. Substituting (18) into (17) yields the following first-order linearized expression:

$$2\,\Re\{Tr(X_i^H J_i^{-1} X(\tilde{t}))\} \approx 2\,\Re\{Tr\left((G_I^{(i)})^H \Delta H\right)\}, \quad (19)$$

where $G_I^{(i)} = SH_i(WK^H + KW^H)$ and $K = J_i^{-1}X_i$. Based on the chain rule, the channel variation owing to the change in the MA position is expressed as $\Delta H = F^H \Sigma \Delta G$. When the m-th antenna moves, the corresponding variation is expressed as

$$\Delta G = [0, \ldots, J_m^{(i)} \Delta t_m, \ldots, 0], \quad (20)$$

which yields

$$\Re\{Tr((G_I^{(i)})^H \Delta H)\} = \sum_{m=1}^{M} (g_{I,m}^{(i)})^T \Delta p_m, \quad (21)$$

where

$$g_{I,m}^{(i)} = Re(J_m^{(i)})^H \left(\Sigma^H F G_I^{(i)}\right)(:, m). \quad (22)$$

Here, $J_m^{(i)}$ denotes the Jacobian of the channel matrix with respect to the position of the m-th antenna, representing the spatial sensitivity of the channel. A similar linearization process can be applied to the interference and noise terms, yielding an additional gradient component, $\mathbf{G}_{II}^{(i)}$. The overall gradient vector is defined as

$$h_m^{(i)} = 2\left(g_{I,m}^{(i)} - g_{II,m}^{(i)}\right), \quad (23)$$

where $G_{II}^{(i)}$ accounts for the sensitivity of interference covariance matrix $J(\tilde{p})$, including the residual SI and thermal noise components. Consequently, the strongly concave lower bound of the surrogate function is given as

$$f_{SCA}(\tilde{p} \mid \tilde{p}^i) = \sum_{m=1}^{M} (h_m^{(i)})^T \Delta p_m - \frac{1}{2} \sum_{m=1}^{M} \delta_m^{(i)} \| \Delta p_m \|_2^2, \quad (24)$$

where $\delta_m^{(i)}$ denotes the Lipschitz constant for each block to ensure convergence stability during iterations.

SCA-based linearization for the minimum-distance and communication QoS constraints follows the standard relaxation approach expressed in [7]

IV. Simulation Results

A. Simulation setup

In our numerical configuration, the BS is located at (0, 0), the UAV-mounted RIS at (20 m, 30 m), and the target at (40 m, 30 m). Two users are uniformly distributed in the region (30 m, 0) to (30 m, 40 m). The BS–RIS and RIS–user links follow Rician fading, whereas BS–user links experience Rayleigh fading with 15 dB shadowing. The initial MA positions are generated by the circle-packing method [6].

B. Performance evaluation

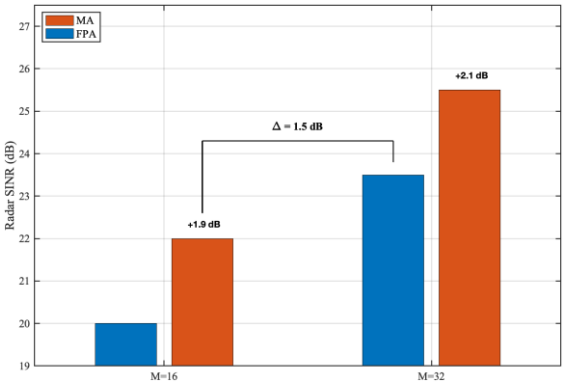

Fig. 2. Comparison of final converged radar SINR between MA and FP A.

Fig. 2 quantitatively compares the final converged radar SINR values of the MA and FPA schemes. When $M = 16$, the MA outperforms the FPA by approximately 1.9 dB, and when $M = 32$, by about 2.1 dB.

Remarkably, the $M = 16$ MA configuration achieves an SINR only 1.5 dB lower than the $M = 32$ FPA, corresponding to an effective 1.6-fold power gain. This implies that employing MAs can yield performance comparable to physically increasing the antenna count while reducing hardware complexity and cost. Moreover, the consistent MA gain across different M values indicates that its improvement is structurally robust and not sensitive to array scale.

V. Conclusion

This paper investigated an active RIS- and movable antenna-aided ISAC system for enhancing radar sensing performance in non-terrestrial networks. An SCA-based optimization framework was developed to adapt MA positions, effectively improving radar SINR under communication constraints. Simulation results showed that movable antennas consistently outperform fixed arrays, achieving comparable sensing performance with fewer antenna elements. These results highlight the effectiveness of MA as a key degree of freedom in active RIS-assisted ISAC systems.

Acknowledgment

"This work was supported by the Institute of Information & Communications Technology Planning & Evaluation (IITP)-Innovative Human Resource Development for Local Intellectualization program grant funded by the Korea government (MSIT: Ministry of Science and ICT) (IITP-2025-RS-2022-00156287)." "This research was supported by the Ministry of Science and ICT (MSIT), Korea, under the ICT Challenge and Advanced Network of HRD (ICAN) support program supervised by the Institute for Information & Communications Technology Planning & Evaluation (IITP) (IITP-2025-RS-2022-00156385)." "This work was supported by the National Research Foundation of Korea (NRF) grant funded by the Korea government (MSIT: Ministry of Science and ICT) (RS-2023-00220985), (RS-2023-00246381), and (RS-2024-00333826)."

References

[1] G. Liu et al., "Cooperative sensing for 6G ISAC: Concept, key technologies, performance evaluation, and field trial," Engineering, 2025, doi: 10.1016/j.eng.2025.08.033.

[2] S. Moon, C.-G. Lee, and I. Hwang, "Secrecy rate maximization for RIS-assisted UAV-ISAC systems," Journal of the Institute of Electronics and Information Engineers, vol. 61, no. 11, pp. 3–10, Nov. 2024, doi: 10.5573/ieie.2024.61.11.3.

[3] S. Rubab, G. E. M. Abro, H. Mustafa, S. K. Baloch, S. A. Memon, and N. Saeed, "RIS-assisted UAV communications: A review of system models, frameworks and outage performance," ICT Express, 2025, doi: 10.1016/j.icte.2025.10.006.

[4] Md. Saiam, M. Z. Chowdhury, S. R. Hasan, and Y. M. Jang, "Reconfigurable intelligent surface assisted BackCom: An overview, analysis, and future research directions," ICT Express, vol. 9, no. 5, pp. 927–940, Oct. 2023, doi: 10.1016/j.icte.2023.07.004.

[5] Z. Yu, H. Ren, C. Pan, G. Zhou, B. Wang, M. Dong, and J. Wang, "Active RIS-aided ISAC systems: Beamforming design and performance analysis," IEEE Transactions on Communications, vol. 72, no. 3, pp. 1578–1592, Mar. 2024, doi: 10.1109/TCOMM.2023.3332856.

[6] X. Gao, J. Xu, Y. Liu, D. W. K. Ng, and M. D. Renzo, "Movable antenna-enabled RIS-aided integrated sensing and communication," IEEE Transactions on Wireless Communications, vol. 23, no. 8, pp. 10540–10555, Aug. 2024, doi: 10.1109/TWC.2024.3352953.

[7] B. Lyu, Y. Bi, Y. Liu, Y. Feng, and H. Hu, "Sum-rate optimization for movable antenna enabled wireless powered communication network," ICT Express, 2025, doi: 10.1016/j.icte.2025.10.005.